# From GTMDs to GPDs: Worldsheet Factorization with Strings Attached

## Fixed-spin holographic amplitudes, Wilson-line worldsheets, and parton tomography in the EIC era

**Kiminad Mamo**
University of Connecticut

Light Cone 2026: Applications at EIC era
Center for Frontiers in Nuclear Science, Stony Brook University

June 23, 2026

# This talk builds on four fixed-spin results

## All-skewness GPD moments

**KM and I. Zahed**,
Phys. Rev. Lett. **133**, 241901 (2024),
arXiv:2411.04162.
*String parametrization of quark and gluon conformal moments.*

## Open/closed $\leftrightarrow \pm$ basis

**KM**, arXiv:2604.12038 (2026).
*Fixed-scale structural matching of holographic open/closed exchange to the singlet eigenbasis.*

## Vacuum source $\rightarrow$ hadronic kernel

**KM**, arXiv:2604.12037 (2026).
*The vacuum-normalized current source produces the fixed-j conformal kernel inside a hadron.*

## Finite-$b_T$ gluon GTMD

**KM and I. Zahed**, arXiv:2606.20981 (2026).
*Fixed-spin worldsheet factorization, transverse endpoints, and Reggeization.*

## Today's synthesis

DVCS factorization $\rightarrow$ conformal moments $\rightarrow$ Witten diagrams $\rightarrow$ string GPDs $\rightarrow$ worldsheet-dressed GTMDs/Wigner distributions.

# One fixed-spin architecture

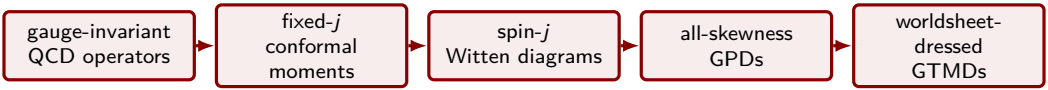


**Same fixed-$j$ string exchange—now with a Wilson-line worldsheet attached.**

GTMDs are the parent correlators in the tomography hierarchy, but the calculation proceeds from constrained GPD conformal moments to their finite-$b_T$ worldsheet dressing.

1. DVCS in $x$-space is an ill-posed inverse problem.
2. The conformal $\pm$ basis turns the unknowns into physical operator moments.
3. The AdS upper vertex reproduces the same hypergeometric hard kernel.
4. String moments give GPDs; a staple worldsheet supplies the finite-$b_T$ GTMD dressing.

## Thesis

The conformal-spin label $j$ is the common language of the light-cone OPE, polynomial GPD moments, holographic exchange, and the Wilson-line worldsheet.

# Physical QCD probes are gauge-invariant color singlets

## Operational statement for spectroscopy and scattering

Physical hadrons are interpolated by gauge-invariant color-singlet operators; measurable structure is encoded in their correlation functions and off-forward matrix elements.

### Local currents

$$J^\mu = \bar{q}\gamma^\mu q, \qquad T^{\mu\nu},$$

$$\mathcal{O}_j^q \sim \bar{q}\gamma^+(iD^+)^{j-1}q.$$

charges, form factors, twist-two moments

### Straight-link bilocals

$$\bar{q}\left(-\frac{z}{2}\right)\gamma^+ W\left[-\frac{z}{2},\frac{z}{2}\right] q\left(\frac{z}{2}\right)$$

PDFs and GPDs on the light front

### Staple-link bilocals

$$\mathrm{Tr}\left[F^{+i}(0)U_{\mathrm{st}}(0,y)F_i^+(y)U_{\mathrm{st}}(y,0)\right]$$

TMDs and GTMDs; rapidity and soft structure

Colored partons are useful internal degrees of freedom; physical asymptotic states and observables are gauge invariant.

# The tomography hierarchy is an operator hierarchy

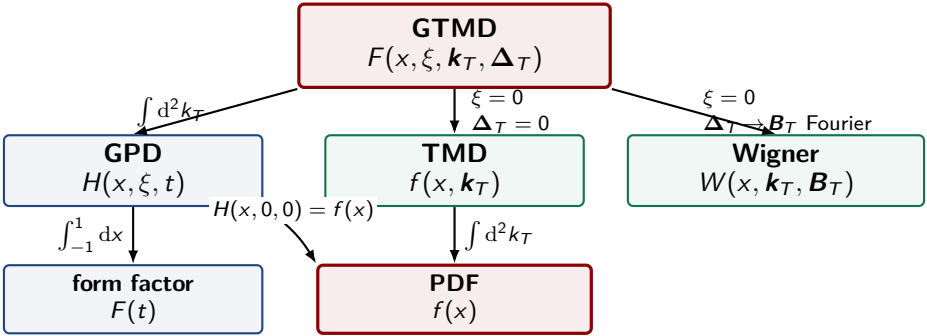


## Two different transverse coordinates

$\boldsymbol{B}_T \longleftrightarrow \boldsymbol{\Delta}_T$ (hadron impact parameter), $\boldsymbol{b}_T \longleftrightarrow \boldsymbol{k}_T$ (partonic separation).

The GTMD retains both the off-forward transfer and the finite transverse separation; the latter is where the staple-link rapidity structure lives.

# Holographic dictionary in light-cone language

| QCD boundary object | Holographic bulk object |
|---|---|
| hadron state $\lvert P\rangle$ | normalizable wave function $\Psi_P(z)$ |
| current $J^\mu$ | bulk gauge field $\mathcal{V}^\mu(Q,z)$ |
| local twist-two $\mathcal{O}_j$ | spin-$j$ bulk field / string trajectory |
| Wilson line or staple | classical string worldsheet |
| operator correlator | Witten diagram |
| analytic continuation in $j$ | Reggeized string exchange |

## Generating functional

$$Z_{\rm holo}[J] \simeq \exp\big(iS_{\rm 5D}^{\text{on-shell}}[\phi|_{z=0}=J]\big)\,,$$

$$\langle \mathcal{O}_1 \cdots \mathcal{O}_n\rangle = \frac{\delta^n S_{\text{on-shell}}}{\delta J_1 \cdots \delta J_n}.$$

## Radial intuition

$z \sim 1/Q$ is ultraviolet resolution;
$z \sim 1/\Lambda_{\rm QCD}$ is hadronic structure and confinement.

This is a holographic-QCD model of the relevant correlators.

# From the vacuum current correlator to a current correlator inside a hadron

**vacuum two-point function**

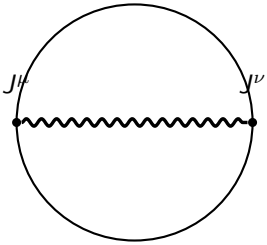


$\mathcal{V}(Q, z)$ fixes the UV current normalization $g_5$

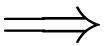

**hadronic current correlator**

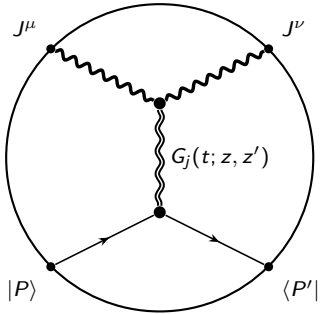


same photon source above; spin-$j$ hadronic moment below

## Question answered by the matching papers

Does the vacuum-normalized upper Witten vertex produce the same fixed-$j$ hard kernel as the QCD conformal OPE? Yes, after the stated TT projection and at one matching scale.

# DVCS: a current-current correlator on the light front

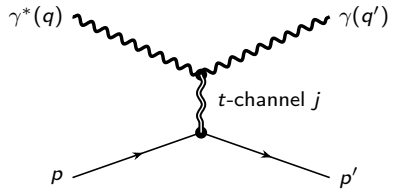


$q^2 = -Q^2, \qquad \Delta = p' - p, \qquad t = \Delta^2,$

$\xi \simeq \dfrac{x_B}{2 - x_B}$ in the Bjorken limit.

## Compton tensor

$$T^{\mu\nu} = \mathrm{i} \int \mathrm{d}^4 z \, \mathrm{e}^{-\mathrm{i} q \cdot z} \langle p' | T\{J^\mu(z/2) J^\nu(-z/2)\} | p \rangle .$$

The unpolarized leading-twist CFF is contained in

$$\mathcal{H} \equiv -\frac{1}{2} g_{\mu\nu}^T T^{\mu\nu} + \mathcal{O}\left(\frac{-t}{Q^2}, \frac{M_N^2}{Q^2}\right).$$

## Collinear factorization

$$\mathcal{H} = \sum_{i=q,g} C_i(Q/\mu) \otimes H_i(x, \xi, t; \mu) + \text{power corrections}.$$

# What DVCS measures in $x$-space

At leading order in a standard vector convention,

$$\mathcal{H}(\xi,t) = \int_{-1}^{1} \mathrm{d}x \left[\frac{1}{\xi - x - \mathrm{i}0} - \frac{1}{\xi + x - \mathrm{i}0}\right] H(x,\xi,t).$$

Therefore

$$\Im\mathcal{H}(\xi,t) = \pi\,[H(\xi,\xi,t) - H(-\xi,\xi,t)],$$

while $\Re\mathcal{H}$ is a principal-value integral plus a subtraction contribution.

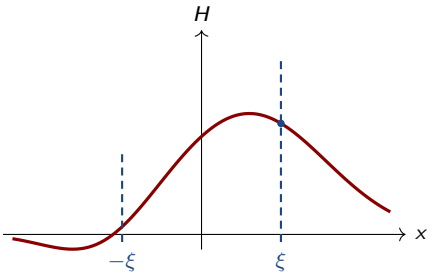

imaginary part samples the crossover line

## Key point

The measured CFF is a weighted projection of a two-variable function. It is not a point-by-point photograph of $H(x,\xi,t)$.

Diehl (2003), arXiv:hep-ph/0307382; Belitsky–Radyushkin (2005), arXiv:hep-ph/0504030.

# The GPD deconvolution problem is an ill-posed inverse problem

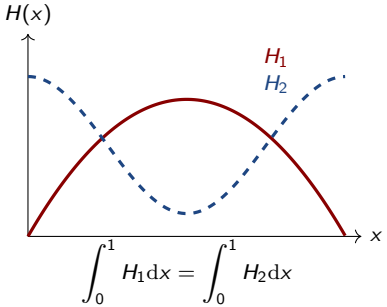


Different shapes can have the same area. DVCS replaces the flat area by a known singular weight $C(x, \xi)$.

## Null directions of the convolution map

$$\delta\mathcal{H}(\xi, t) = \int_{-1}^{1} \mathrm{d}x \; C(x, \xi)\, \delta H(x, \xi, t) \simeq 0$$

can hold for nontrivial $\delta H$ over the measured kinematic range.

- Many $x$-space profiles produce nearly identical CFFs.
- Evolution, NLO information, and additional channels constrain the near-null directions but do not make the map unique.

## Consequence

Flexible $x$-space fits require operator, lattice, and form-factor constraints; otherwise the inverse is unstable.

# Change basis: from a light-ray operator to local conformal operators

## Light-ray OPE

$$\mathcal{O}(z_1, z_2) = \sum_j C_j(z_{12}; \mu)\, \mathcal{O}_j(\mu).$$

For the leading unpolarized sector,

$$\mathcal{O}_j^q \sim \bar{q}\gamma^+ (i \overleftrightarrow{D}^+)^{j-1} q,$$

$$\mathcal{O}_j^g \sim \mathrm{Tr}\left[F^{+i}(iD^+)^{j-2}F_i^+\right].$$

## Finite-skewness conformal moments

$$H_j^q(\eta, t) = \mathcal{N}_j^q \int_{-1}^{1} \mathrm{d}x\, \eta^{j-1} C_{j-1}^{3/2}\left(\frac{x}{\eta}\right) H^q(x, \eta, t),$$

$$H_j^g(\eta, t) = \mathcal{N}_j^g \int_{-1}^{1} \mathrm{d}x\, \eta^{j-2} C_{j-2}^{5/2}\left(\frac{x}{\eta}\right) H^g(x, \eta, t).$$

## Why this basis is physical

Each coefficient is the matrix element of a local twist-two operator with definite spin $j$; it is not an arbitrary expansion coefficient.

# Polynomiality is Lorentz covariance written in moment space

For physical integer spin,

$$\int_{-1}^{1} \mathrm{d}x\, x^{n-1} H(x,\eta,t) = \sum_{k=0}^{n} (2\eta)^k A_{n,k}(t),$$

with only the parity-allowed powers and a highest-power $D$-term contribution.

## What this means

At every spin, skewness dependence is a finite polynomial fixed by the Lorentz decomposition of a local operator matrix element.

The holographic spin projector gives the analytic continuation

$$\widehat{d}_j(\eta,t) = {}_2F_1\left(-\frac{j}{2}, \frac{1-j}{2}; \frac{1}{2} - j; -\frac{4M_N^2\eta^2}{-t}\right).$$

For even physical $j$, this terminates and becomes a finite polynomial in $\eta^2$.

## Separation of roles

Polynomiality belongs to the lower hadronic matrix element. It is not generated by adjusting the hard DVCS coefficient function.

Diehl (2003), arXiv:hep-ph/0307382; Nishio–Watari (2014), arXiv:1408.6365; KM–Zahed (2024), arXiv:2411.04162.

# The singlet $\pm$ basis diagonalizes leading evolution

$$\mu\frac{\mathrm{d}}{\mathrm{d}\mu}\begin{pmatrix} H_j^{\Sigma} \\ H_j^{g} \end{pmatrix} = -\begin{pmatrix} \gamma_j^{\Sigma\Sigma} & \gamma_j^{\Sigma g} \\ \gamma_j^{g\Sigma} & \gamma_j^{gg} \end{pmatrix}\begin{pmatrix} H_j^{\Sigma} \\ H_j^{g} \end{pmatrix}.$$

Define eigenmoments

$$\begin{pmatrix} H_j^{+} \\ H_j^{-} \end{pmatrix} = U_j \begin{pmatrix} H_j^{\Sigma} \\ H_j^{g} \end{pmatrix}, \qquad \mu\frac{\mathrm{d}H_j^{\pm}}{\mathrm{d}\mu} = -\gamma_j^{\pm} H_j^{\pm}.$$

## The first physical even moment

$$\gamma_2^{-} = 0, \qquad \gamma_2^{+} \neq 0.$$

The $(-)$ eigenchannel is protected by the singlet momentum sum rule; the $(+)$ channel is unprotected.

## Important caveat

$H_j^{\pm}$ are mixed quark–gluon eigenchannels at finite $N_c$; they are not literal unmixed "quark" and "gluon" operators.

D. Müller (1998), arXiv:hep-ph/9704406; Belitsky–Müller (1998), arXiv:hep-ph/9709379; Kumerički et al. (2008), arXiv:hep-ph/0703179.

# Fixed-$j$ QCD CFF: hard kernel $\times$ physical moment

Let $\vartheta \equiv \eta/\xi$. In the singlet eigenbasis,

$$\widehat{\mathcal{H}}^{\text{sing}}_{\text{QCD}}(j) = \sum_{a=\pm} \underbrace{\xi^{-j} c_j^a \left(\frac{\mu}{Q}\right)^{\gamma_j^a} \mathcal{K}_j^{(\gamma_j^a)}(\vartheta)}_{\text{hard current kernel}} \underbrace{\left(\frac{\mu_0}{\mu}\right)^{\gamma_j^a} H_j^a(\eta, t; \mu_0)}_{\text{hadronic conformal moment}}.$$

$$\boxed{\mathcal{K}_j^{(\gamma)}(\vartheta) = {}_2F_1\left(\frac{j}{2} + \frac{\gamma}{4}, \frac{j+1}{2} + \frac{\gamma}{4}; j + \frac{3}{2} + \frac{\gamma}{2}; \vartheta^2\right)}$$

## DDVCS

Both photons are off shell: $|\vartheta| < 1$ exposes the full hypergeometric dependence.

## DVCS endpoint

One photon becomes real: $\vartheta \to 1$ and the same kernel reduces to a gamma-function ratio.

KM (2026), arXiv:2604.12037 and arXiv:2604.12038.

# Compute the same fixed-$j$ object as a Witten diagram

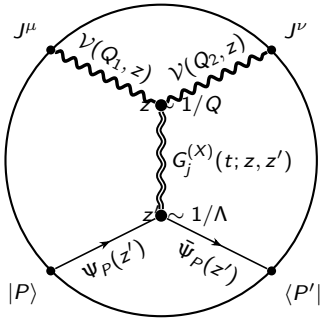


- Fix spin $j$ before the Sommerfeld–Watson / Regge resummation.
- Apply the transverse–transverse scalar projection.
- The upper photon vertex is localized near $z \sim 1/Q$.
- The lower nucleon vertex probes the confining region.

## Holographic collinear intuition

A shallow UV endpoint factorizes from the deep hadronic endpoint: hard kernel $\times$ operator moment.

# Fixed-$j$ Witten factorization: UV kernel, IR moment

When the photon-side endpoint is pushed toward the boundary,

$$G_j^{(X)}(z,z';t) \longrightarrow \Psi_j^{(X),\mathrm{bdry}}(z;\epsilon)\,\mathcal{H}_j^{(X)}(t,z';\epsilon), \qquad X = o, c.$$

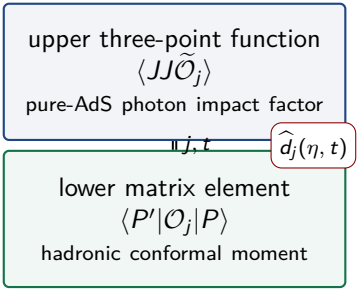


## Upper vertex: universal

Vacuum-normalized photon profile; $z \sim 1/Q$; all hard $Q^2$ and $\eta/\xi$ dependence; the hypergeometric kernel.

## Lower vertex: hadronic

Nucleon wave functions and confinement; $t$ dependence; spin-$j$ form factors; polynomiality through $\widehat{d}_j$.

## Factorized amplitude: hard kernel $\times$ conformal moment

$$\widehat{\mathcal{H}}_{\mathrm{holo}}^{(X)}(j) = \xi^{-j}\left(\frac{\mu}{Q}\right)^{\gamma_X(j)} \mathcal{K}_j^{(\gamma_X(j))}(\eta/\xi)\left(\frac{\mu_0}{\mu}\right)^{\gamma_X(j)} \Phi_N^{(X)}(j;t,\eta).$$

# The UV AdS integral is the conformal Wilson kernel

With conformal photon profiles $\mathcal{V}(Q,z) = QzK_1(Qz)$,

$$C_1(\delta,\vartheta) = \sqrt{1-\vartheta^2}\int_0^\infty \mathrm{d}y\, y^{1+\delta} K_1\big(y\sqrt{1+\vartheta}\big)\, K_1\big(y\sqrt{1-\vartheta}\big)\,,$$

$$C_1(\delta,\vartheta) = N(\delta)\,{}_2F_1\Big(\frac{\delta}{4},\frac{\delta}{4}+\frac{1}{2};\frac{\delta}{2}+\frac{3}{2};\vartheta^2\Big)\,.$$

The Witten-diagram $z$ powers give

$$\underbrace{z^{-5}}_{\text{measure}}\ \underbrace{z^{4+2(j-2)}}_{VV\mathcal{O}_j\text{ tensor vertex}}\ \underbrace{z^{-(j-2)}}_{\text{propagator convention}}\ \underbrace{z^{\Delta_X(j)}}_{\text{boundary mode}}\ \underbrace{z^{2}}_{\text{two photons}} = z^{j+\Delta_X(}$$

## Mellin label

$$\boxed{\delta_X(j) = j + \Delta_X(j) - 2 = 2j + \gamma_X(j)}\,.$$

It is derived from the actual Witten vertex, not inserted as an ansatz.

Open $C_1$: Nishio–Watari (2014), arXiv:1408.6365; closed BPST: KM (2026), arXiv:2604.12037 and arXiv:2604.12038.

# Fixed-scale matching and the protected $j = 2$ anchor

At the single matching point $Q = \mu = \mu_0 = \mu_*$,

$$\gamma_o(j) \overset{\text{kernel}}{\longleftrightarrow} \gamma_j^+, \quad \Phi_N^{(o)}(j;t,\eta) \longleftrightarrow c_j^+ H_j^+(\eta,t;\mu_*),$$
$$\gamma_c(j) \overset{\text{kernel}}{\longleftrightarrow} \gamma_j^-, \quad \Phi_N^{(c)}(j;t,\eta) \longleftrightarrow c_j^- H_j^-(\eta,t;\mu_*).$$

## Closed BPST branch

$$\Delta_c(2) = 4, \qquad \gamma_c(2) = 0$$

because spin two is the conserved total energy–momentum tensor:

$$\boxed{\text{closed} \longleftrightarrow (-) \text{ protected}}.$$

## Even open branch

There is no Ward-identity zero at $j = 2$:

$$\gamma_o(2) \text{ is unprotected}, \qquad \gamma_2^+ \neq 0,$$

so

$$\boxed{\text{open} \longleftrightarrow (+) \text{ unprotected}}.$$

## Scope

This is a TT-projected kernel-and-moment dictionary at one scale. It does not equate weak- and strong-coupling anomalous-dimension functions for all $j$ or all scales. The $\pm$ channels remain mixed quark–gluon eigenchannels at finite $N_c$.

# What the conformal/string strategy buys in the deconvolution problem

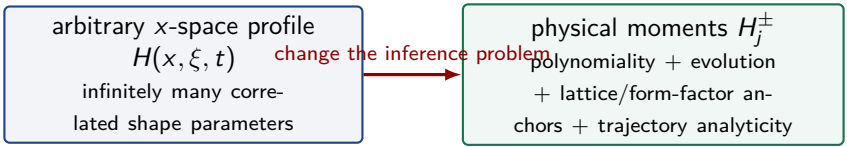


## Unconstrained inversion

The data constrain a small set of convolution projections, leaving large functional null directions.

## Constrained operator inference

Fit matrix elements of definite-spin operators whose skewness dependence and evolution are already restricted.

## Precise claim

This is an effective cure / regularization of the practical GPD extraction problem. It does *not* prove that DVCS data alone make the inverse map mathematically injective; complementary channels remain indispensable.

Bertone et al. (2021), arXiv:2104.03836; KM (2026), arXiv:2604.12037 and arXiv:2604.12038.

# String parametrization of all-skewness conformal moments

The moment is organized as a spin-$j$ $A$-form factor plus its skewness-dependent $D$-form-factor completion,

$$H_j^i(\eta, t; \mu_0) = A_j^i(t; \mu_0) + \mathcal{D}_j^i(\eta, t; \mu_0), \qquad i = q, g.$$

In the holographic string representation, schematically,

$$\mathcal{D}_j^i(\eta, t) \propto [\widehat{d}_j(\eta, t) - 1]\,[A_j^i(t) - A_{S,j}^i(t)].$$

- $A_j^i(0)$ is anchored by empirical PDF moments.
- $t$ dependence is controlled by open/closed Regge slopes and form-factor data.
- The finite polynomial $\widehat{d}_j$ enforces all-skewness Lorentz structure.

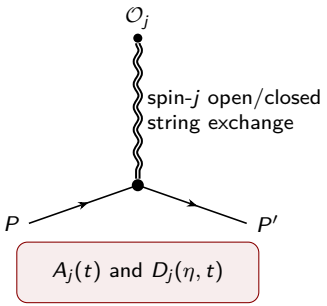


**Few-parameter architecture**

The implementation uses a small set of Regge-slope parameters rather than a free function of $(x, \xi, t)$.

KM–Zahed (2024), Phys. Rev. Lett. 133, 241901, arXiv:2411.04162.

# From conformal moments back to $H(x, \eta, t)$

## Mellin–Barnes / Sommerfeld–Watson reconstruction

$$H(x, \eta, t; \mu) = \frac{1}{2\mathrm{i}} \int_{c-\mathrm{i}\infty}^{c+\mathrm{i}\infty} \mathrm{d}j \, \frac{p_j(x, \eta)}{\sin(\pi j)} \, H_j(\eta, t; \mu),$$

with the appropriate even/odd signature factor and quark/gluon conformal partial wave $p_j$.

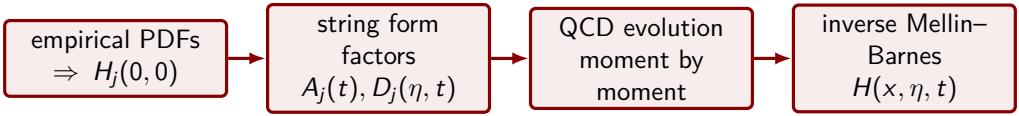


## Built in

Support, polynomiality, crossing/signature, analytic continuation in $j$.

## Fitted or matched

Forward moments, Regge slopes, confinement scales, and finite normalization factors.

# All-skewness GPDs: the deliverable

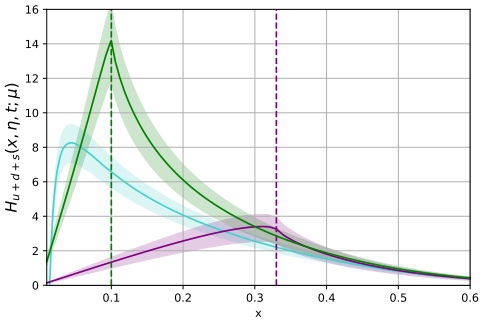


Unpolarized singlet quark GPD

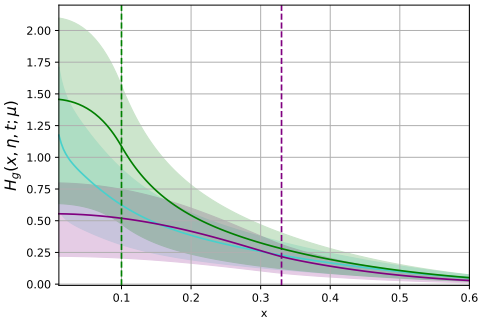


Symmetric unpolarized gluon GPD

## What is controlled

The dashed crossover boundaries $|x| = \xi$, the ERBL/DGLAP continuation, and the moment polynomiality all come from the same conformal partial-wave representation.

KM–Zahed (2024), Phys. Rev. Lett. 133, 241901, arXiv:2411.04162.

# From a gluon GPD to a gluon GTMD: what is added?

## Straight-link gluon GPD operator

For $z_T = 0$,

$$\mathcal{O}_g^{\mathrm{str}}(z) = \mathrm{Tr}\left[F^{+i}\left(-\frac{z}{2}\right) U_{\mathrm{str}} F_i^{+}\left(\frac{z}{2}\right) U_{\mathrm{str}}^{\dagger}\right],$$

$$H^g(x,\xi,t) \sim \int \mathrm{d}z^- \, \mathrm{e}^{\mathrm{i}x\bar{P}^+ z^-} \langle P'|\mathcal{O}_g^{\mathrm{str}}(z)|P\rangle.$$

The average partonic $\boldsymbol{k}_T$ is integrated out.

## Staple-link gluon GTMD operator

For $z_T = \boldsymbol{b}_T$,

$$\mathcal{O}_g^{\mathrm{st}}(z, b_T) = \mathrm{Tr}\left[F^{+i}\left(-\frac{z}{2}\right) U_{\mathrm{st}} F_i^{+}\left(\frac{z}{2}\right) U_{\mathrm{st}}^{\dagger}\right],$$

$$F^g(x,\xi,\boldsymbol{k}_T,\boldsymbol{\Delta}_T) \longleftrightarrow F^g(x,\xi,t,\boldsymbol{b}_T).$$

The staple adds rapidity geometry and a soft factor.

## Fixed-spin simplification

The operator logic is general; from here onward I specialize to the C-even gluon channel. A conformal moment collapses the longitudinal light ray to a local spin-$j$ operator, leaving the transverse separation $\boldsymbol{b}_T$ on the staple worldsheet.

# Gauge-invariant gluon GTMD on the light front

For $y = (0, y^-, \boldsymbol{b}_T)$,

$$\mathcal{O}_g(y) = \mathrm{Tr}\big[F^{+i}(0) U_{\mathrm{st}}(0,y) F^+_i(y) U_{\mathrm{st}}(y,0)\big] .$$

The even-spin gluon conformal moment is

$$\mathbb{F}^g_j(\xi, t, b_T) = \mathcal{N}^g_j \int_{-1}^{1} \mathrm{d}x\, \xi^{j-2} C^{5/2}_{j-2}\!\left(\frac{x}{\xi}\right) \times F_g(x, \xi, t, b_T), \qquad j = 2, 4, \ldots$$

with $\mathbb{F}^g_j(0, t, b_T) = \int \mathrm{d}x\, x^{j-2} F_g$ in the zero-skewness limit $\xi \to 0$.

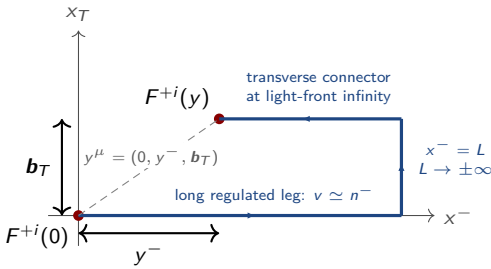


$U_{\mathrm{st}}(y, 0)$ retraces the same regulated contour in reverse.

## New scales

The long legs follow an off-light-cone regulator direction $v \simeq n^-$, introducing the rapidity scale $\zeta$ in addition to ordinary UV renormalization at $\mu$.

# “Strings attached” is literal

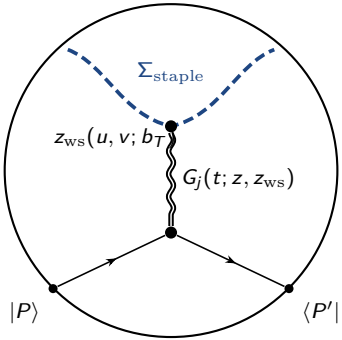


**Same closed spin-$j$ channel as the gluon GPD moment.**

- The boundary staple is the endpoint of a classical string worldsheet.
- The bilocal operator sources the spin-$j$ field over that worldsheet.
- The spin-$j$ field propagates to the same hadron-side Witten vertex used in the GPD sector.

## Geometric statement

The GTMD is obtained by attaching a Wilson-line worldsheet to the fixed-spin exchange whose boundary limit already defines the GPD conformal moment.

# Leading-saddle worldsheet factorization

The strict local and finite-separation sectors are piecewise:

$$F_j^g(\xi,t,0;\mu,\zeta) = \widetilde{F}_j^{g,\mathrm{bdry}}(\xi,t;\mu),$$
$$F_j^g(\xi,t,b_T;\mu,\zeta) = S(b_T;\mu,\zeta)\,\widetilde{F}_j^{g,\mathrm{ws}}(\xi,t,b_T;\mu) + \mathcal{O}(N_c^{-2},\lambda^{-1/2}), \qquad b_T > 0.$$

Convention: $S^{1/2}$ denotes one staple factor; $S = (S^{1/2})^2$ denotes the two-staple factor.

## Universal vacuum factor

$$S^{1/2}(b_T;\mu,\zeta) = \exp[-S_{\mathrm{NG}}(\Sigma^{\min}_{\mathrm{staple}})].$$

It depends on the staple geometry, cusp regulator, and background.

## Target-dependent stripped amplitude

$$\widetilde{F}_j^{g,\mathrm{ws}} = \int \mathrm{d}z\mathrm{d}z'\, J^{(j)}_{\mathrm{had}}(\xi,t;z)\,G_j(z,z';t)\,J^{(j)}_{\mathrm{op}}(b_T;z').$$

## Separate saddle sectors

The strict point $b_T = 0$ is a boundary/contact Witten diagram. The endpoint $b_T \to 0^+$ of the finite-separation worldsheet saddle is not by itself the perturbative small-$b_T$ OPE.

# Endpoint reductions at a glance

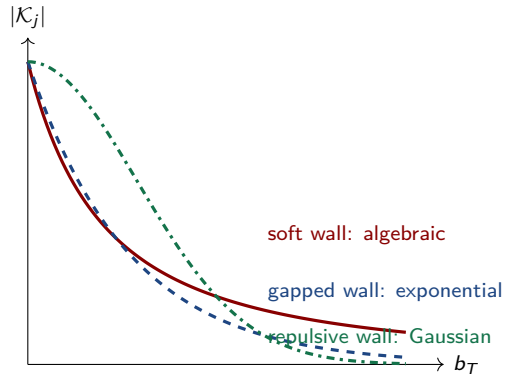


## UV overlap

$$\widetilde{F}_j^{g,\mathrm{ws}} \to \mathcal{K}_j^{\mathrm{UV}}(b_T)\,\widetilde{F}_j^{g,\mathrm{bdry}}, \qquad \mathcal{K}_j^{\mathrm{UV}} \sim \bar{b}^{\,4+\gamma_c(j)}.$$

## IR transfer

$$\mathcal{K}_j^{\mathrm{IR,SW}} \sim \bar{b}^{\,2-j-a_{t,c}},$$

$$\mathcal{K}_j^{\mathrm{IR,gap}} \sim (\kappa_{\mathrm{IR}} b_T)^{\frac{7}{2}-j} \mathrm{e}^{-\kappa_{\mathrm{IR}} b_T}.$$

## Universal statement vs model data

The radial endpoint logic and the UV overlap are universal at leading saddle. The detailed large-$b_T$ tail diagnoses the chosen infrared completion.

# Future parametrization: dress the fitted GPD moments

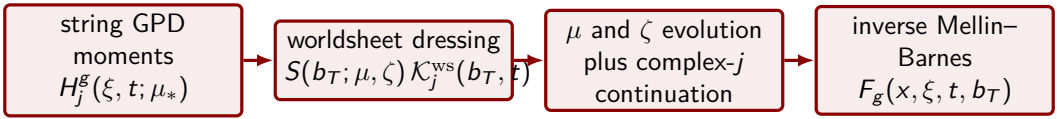


$$F_j^g(\xi, t, b_T; \mu, \zeta) \sim S(b_T; \mu, \zeta)\, \mathcal{K}_j^{\rm ws}(b_T, t)\, H_j^g(\xi, t; \mu) \quad \text{(piecewise saddle architecture).}$$

## Boundary data already available

PDF moments, all-skewness GPD moments, electromagnetic / gravitational form factors, lattice constraints.

## New GTMD information

Rapidity soft factor, nonperturbative $b_T$ dressing, infrared correlation length, and BPST diffusion.

## Phenomenological target

Promote the existing string-GPD fits into candidate GTMD parametrizations for EIC exclusive channels. Reggeization introduces no additional function beyond the fixed-$j$ GTMD input: it analytically continues the same worldsheet-dressed conformal moments into the low-$x$ regime.

# Take-home messages

1. Gauge-invariant local and bilocal color-singlet operators define the measurable QCD correlators.
2. Fixed conformal spin turns DVCS into physical moments with manifest polynomiality and diagonal singlet evolution.
3. The UV Witten vertex is the conformal hard kernel; the IR lower vertex is the hadronic moment.
4. String-parametrized moments regularize the otherwise underconstrained $x$-space deconvolution problem.
5. Attaching the staple worldsheet adds rapidity evolution and finite-$b_T$ structure; complex-$j$ continuation gives the low-$x$ regime.

**Same fixed-$j$ string exchange—now with a Wilson-line worldsheet attached.**

# Thank you

**From DVCS deconvolution to GTMD tomography**

one fixed-$j$ operator basis, one holographic exchange architecture

Questions?

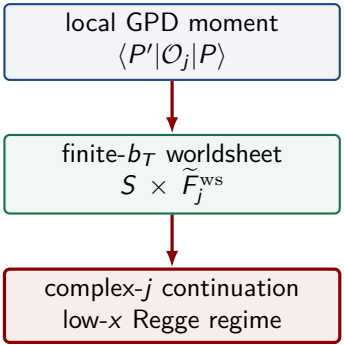


Same fixed-$j$ string exchange—with strings literally attached.

# Backup: exact fixed-$j$ dictionary in one line

$$\widehat{\mathcal{H}}^{(X)}_{\rm holo}(j) = \xi^{-j}\left(\frac{\mu}{Q}\right)^{\gamma_X(j)} \mathcal{K}_j^{(\gamma_X(j))}(\vartheta)\left(\frac{\mu_0}{\mu}\right)^{\gamma_X(j)} \phi_0^X(j)\widehat{d}_j(\eta,t)\mathfrak{g}_X\widehat{\mathcal{F}}_N^{(X)}(j;t), \quad X=o,c.$$

At $Q=\mu=\mu_0=\mu_*$,

$$\gamma_o(j) \longleftrightarrow \gamma_j^+, \qquad \phi_0^o\widehat{d}_j\widehat{\mathcal{F}}_N^{(o)} \longleftrightarrow c_j^+ H_j^+,$$
$$\gamma_c(j) \longleftrightarrow \gamma_j^-, \quad \phi_0^c\widehat{d}_j\left(\frac{\widetilde{g}_5^2}{g_5^2}\right)\widehat{\mathcal{F}}_N^{(c)} \longleftrightarrow c_j^- H_j^-.$$

## Normalization

Only the products $c_j^\pm H_j^\pm$ are basis-normalization invariant. Source normalizations and eigenvector normalizations must be matched consistently.

# Backup: DVCS endpoint of the universal kernel

At $\vartheta \to 1$,

$$ {}_2F_1\left(\frac{\delta}{4}, \frac{\delta}{4}+\frac{1}{2}; \frac{\delta}{2}+\frac{3}{2}; 1\right) = \frac{\Gamma\left(\frac{\delta}{2}+\frac{3}{2}\right)}{\Gamma\left(\frac{\delta}{4}+1\right)\Gamma\left(\frac{\delta}{4}+\frac{3}{2}\right)}, $$

because $c - a - b = 1$ for this hypergeometric family.

## Interpretation

DDVCS displays the full $\eta/\xi$ dependence; DVCS samples the endpoint of the same conformal partial wave. No new hard kernel is introduced when one photon becomes real.

# Backup: detailed $j = 2$ branch assignment

## Closed BPST branch

$$\Delta_c(2) = 4, \qquad \gamma_c(2) = 0.$$

The spin-2 bulk graviton is dual to the conserved total energy–momentum tensor:

$$\text{closed} \quad \longleftrightarrow \quad (-).$$

## Even open branch

$\gamma_o(2)$ has no Ward-identity zero.

The branch is unprotected and therefore maps to

$$\text{open} \quad \longleftrightarrow \quad (+).$$

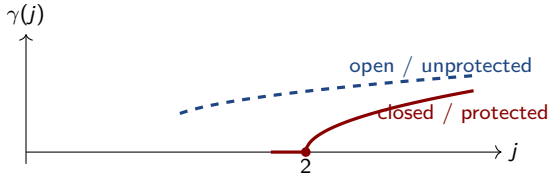


Open/closed denote effective diagonal branches of the projected large-$N_c$ amplitude, not literal pure-quark/pure-gluon operators at finite $N_c$.

# Backup: endpoint factorization formulas

## UV: $b_T \to 0^+$

Worldsheet endpoint is shallower:

$$\widetilde{F}_j^{g,\mathrm{ws}} \to \mathcal{K}_j^{\mathrm{UV}}(b_T)\,\widetilde{F}_j^{g,\mathrm{bdry}}(\xi,t),$$

$$\mathcal{K}_j^{\mathrm{UV}} \sim \bar{b}^{\,4+\gamma_c(j)}, \qquad \bar{b} = \sqrt{2}\kappa_c b_T$$

universal within the leading saddle

## IR: soft wall

Target endpoint is shallower:

$$\widetilde{F}_{j,\mathrm{IR,SW}}^{g,\mathrm{ws}} \to \mathcal{K}_j^{\mathrm{IR,SW}}(b_T,t)\,\widehat{\mathcal{T}}_j^{(c)}(\xi)$$

$$\mathcal{K}_j^{\mathrm{IR,SW}} \sim \bar{b}^{\,2-j-a_{t,c}}.$$

algebraic transfer tail

## IR: gap-matched wall

$$\widetilde{F}_{j,\mathrm{IR,HW}}^{g,\mathrm{ws}} \to \mathcal{K}_j^{\mathrm{IR,HW}}(b_T)\,\widehat{\mathcal{T}}_j^{(c)}(\xi),$$

$$\mathcal{K}_j^{\mathrm{IR,HW}} \sim (\kappa_{\mathrm{IR}} b_T)^{\frac{7}{2}-j} \mathrm{e}^{-\kappa_{\mathrm{IR}} b_T}.$$

finite transverse correlation length

## Universal statement vs model data

The radial endpoint logic and the UV overlap are universal at leading saddle. The detailed large-$b_T$ tail depends on the chosen infrared completion.

# Backup: Reggeization of the same fixed-spin amplitudes

At small $x$,

$$F_g(x,t,b_T) = \frac{1}{2\pi \mathrm{i}} \int_{c-\mathrm{i}\infty}^{c+\mathrm{i}\infty} \mathrm{d}j\, x^{-(j-1)}\, \mathcal{I}_j(t,b_T),$$

$$\mathcal{I}_j(t,b_T) \equiv S(b_T)\, \widetilde{F}_j^{g,\mathrm{ws}}(0,t,b_T).$$

The BPST rightmost branch point is

$$\boxed{j_0^g = 2 - \frac{2}{\sqrt{\lambda}}}.$$

Near the cut, with $Y = \ln(1/x)$ and $\ell_b = \ln(1/\bar{b})$,

$$F_g \sim x^{-(j_0^g-1)} \frac{\mathrm{e}^{-\frac{\sqrt{\lambda}}{2Y}\ell_b^2}}{Y^{3/2}} \times [\text{smooth impact factor}].$$

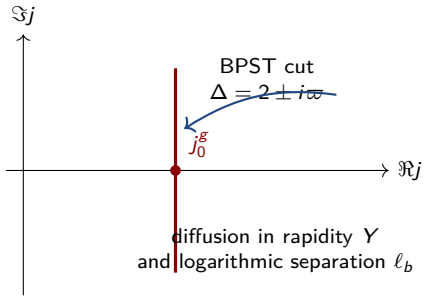


**No new nonperturbative input**

The low-$x$ amplitude is the analytic continuation of the same fixed-$j$ GPD/GTMD moments and transverse kernels.

# Backup: why $b_T = 0$ and $b_T \to 0^+$ are different saddle sectors

$$F_j^g(\xi, t, 0) = \widetilde{F}_j^{g,\mathrm{bdry}}(\xi, t),$$

while for the finite-separation saddle

$$\widetilde{F}_j^{g,\mathrm{ws}}(\xi, t, b_T) \xrightarrow[b_T \to 0^+]{} \mathcal{K}_j^{\mathrm{UV}}(b_T)\widetilde{F}_j^{g,\mathrm{bdry}}(\xi, t), \qquad \mathcal{K}_j^{\mathrm{UV}} \sim \bar{b}^{4+\gamma_c(j)}.$$

Thus, for $\Re[4 + \gamma_c(j)] > 0$,

$$\lim_{b_T \to 0^+} \widetilde{F}_j^{g,\mathrm{ws}} = 0, \qquad F_j^g(\xi, t, 0) = \widetilde{F}_j^{g,\mathrm{bdry}} \neq 0.$$

## No contradiction with perturbative matching

The perturbative small-$b_T$ OPE concerns a fully subtracted operator in a weak-coupling short-distance regime. The statement above concerns the endpoint of one strong-coupling classical worldsheet saddle.

# Backup: leading small-$x$, small-$b_T$ diffusion form

In the BPST diffusion window,

$$F_g(x,t,b_T) \simeq \mathcal{N}_g^{\mathrm{UV}}(t)\, x^{-\left(1-2/\sqrt{\lambda}\right)} S(b_T;\mu,\zeta)\, \bar{b}^{4-j_0^g} \frac{\lambda^{1/4}}{\sqrt{2\pi}\, Y^{3/2}} \left(1-\sqrt{\lambda}\frac{\ell_b^2}{Y}\right) \exp\left[-\frac{\sqrt{\lambda}}{2}\frac{\ell_b^2}{Y}\right],$$

$$Y = \ln(1/x), \qquad \ell_b = \ln(1/\bar{b}), \qquad j_0^g = 2 - \frac{2}{\sqrt{\lambda}}.$$

## Validity

$Y \gg 1$, $0 < \bar{b} \ll 1$, and the saddle remains within the BPST diffusion domain.